Coherent oscillations in monkey motor cortex and hand muscle EMG show task-dependent modulation

S. N. Baker, E. Olivier and R. N. Lemon

*Sobell Department of Neurophysiology, Institute of Neurology, Queen Square,
London WC1N 3BG, UK*

1. Recordings were made of local field potential (slow waves) and pyramidal tract neurone (PTN) discharge from pairs of sites separated by a horizontal distance of up to 1·5 mm in the primary motor cortex of two conscious macaque monkeys performing a precision grip task.

2. In both monkeys, the slow wave recordings showed bursts of oscillations in the 20–30 Hz range. Spectral analysis revealed that the oscillations were coherent between the two simultaneously recorded cortical sites. In the monkey from which most data were recorded, the mean frequency of peak coherence was 23·4 Hz.

3. Coherence in this frequency range was also seen between cortical slow wave recordings and rectified EMG of hand and forearm muscles active during the task, and between pairs of rectified EMGs.

4. The dynamics of the coherence were investigated by analysing short, quasi-stationary data segments aligned relative to task performance. This revealed that the 20–30 Hz coherent oscillations were present mainly during the hold phase of the precision grip task.

5. The spikes of identified PTNs were used to compile spike-triggered averages of the slow wave recordings. Oscillations were seen in 11/17 averages of the slow wave recorded on the same electrode as the triggering spike, and 11/17 averages of the slow wave recorded on the distant electrode. The mean period of these oscillations was 45·8 ms.

6. It is concluded that oscillations in the range 20–30 Hz are present in monkey motor cortex, are coherent between spatially separated cortical sites, and encompass the pyramidal tract output neurones. They are discernable in the EMG of active muscles, and show a consistent task-dependent modulation.

A number of recent studies have reported oscillatory activity in the cerebral cortex, in the range 20–50 Hz. Initial reports in the visual cortex (Singer & Gray, 1995, for review) showed that these oscillations appeared following a specific pattern of stimuli, and that coherence between oscillations at spatially separate sites could be interpreted as having a role in the perceptual 'binding' of stimulus attributes. Murthy & Fetz (1992, 1997*a*) and Sanes & Donoghue (1993) recorded oscillations in local field potentials in the primary motor cortex during the performance of a variety of tasks. These oscillations were most pronounced in the bandwidth 25–35 Hz. Murthy & Fetz (1992, 1997*a*) did not find any consistent modulation with an overtrained wrist flexion–extension task, but reported that the oscillations were strongest during performance of novel tasks, including use of fine finger movements to retrieve small food rewards that were out of the monkey's sight. Sanes & Donoghue (1993) found that oscillations were consistently present while monkeys held their wrist in a target zone, but declined markedly just before and during wrist movement

to another pre-cued wrist position. Oscillations persisted somewhat longer in a task requiring the monkey to press a force plate with its digits. Oscillations were widespread in motor cortex, and synchronized over large distances (up to 14 mm; Murthy & Fetz, 1992, 1997*a*).

A recent report by Conway *et al.* (1995) has demonstrated coherence in the 15–35 Hz range between magneto-encephalographic (MEG) signals recorded over human primary motor cortex, and EMG recorded from hand muscles during a steady-state contraction. This result may reflect functional linkages between motor cortex neurones and motoneurones supplying the hand muscles. In the monkey, motor cortical neurones with outputs to the spinal cord undergo very pronounced modulation in their activity during skilled hand tasks such as the precision grip (Lemon, Mantel & Muir, 1986; Bennett & Lemon, 1996). We have therefore searched for coherence between oscillations in cortical slow wave activity and EMG activity during precision grip. We demonstrate that such coherence is clearly present, that it is strongly modulated during the

task, and that this coherent activity includes identified motor cortex output neurones.

A preliminary report has been published previously (Baker, Olivier & Lemon, 1996).

METHODS

Behavioural task

The results reported here were gathered from cortical and EMG recordings made in two purpose-bred macaque monkeys (both adult females, one *Macaca nemestrina*, one *M. mulatta*) trained to do the precision grip task (Lemon *et al.* 1986) for a fruit reward. Confirmatory analysis of EMG data was carried out on recordings obtained from a further four macaques (one male, three females, all *M. nemestrina*), also performing the precision grip task. The task required that two independently pivoted levers were squeezed between index finger and thumb, and held in electronically defined position windows for around 1 s. Performance on the task was cued to the animal by three tones. The first indicated that the levers were in target, the second that they had been held for long enough and should be released, and the third that a reward would follow. The onset of the second tone ('End hold') was used as a trigger in the analysis of task-related effects.

Surgery

After the animal reached a high level of performance (*ca* 1000 trials per experimental session), it was implanted under general anaesthesia (isoflurane in $50:50$ $O_2:N_2O$) and aseptic conditions with a stainless steel headpiece to allow head fixation, and a circular chamber positioned over the hand representation of area 4 of the left hemisphere. During the same surgery, two fine epoxy insulated tungsten wire electrodes (impedance 15–25 kΩ at 1 kHz) were also implanted in the ipsilateral medullary pyramid, at stereotaxic co-ordinates A3 and P2. Their location was confirmed during the surgery by the presence of an antidromic field potential recorded from the surface of the motor cortex following stimulation through the electrodes, and by post-mortem histology. Antibiotics (20 mg kg^{-1} I.M. Terramycin LA; Pfizer, Sandwich, Kent, UK) and an analgesic (5–10 μg kg^{-1} I.M. Vetergesic (buprenorphine hydrochloride); Reckitt & Colman, York, UK) were administered for the first 2–3 postoperative days. All procedures were carried out under appropriate licences from the UK Home Office.

At the conclusion of recordings in the left hemisphere, the animal was retrained to perform the task with the left hand, and further surgery carried out in which a chamber and pyramidal electrodes were implanted on the right side.

Recording

At the start of each experimental session, the monkey was prepared to record EMG from up to seven hand and forearm muscles. Muscles abductor pollicis brevis (AbPB), adductor pollicis (AdP) and flexor digitorum profundis (FDP) were recorded from intramuscular electrodes inserted percutaneously into the muscle using a hypodermic needle at the start of each session (Lemon *et al.* 1986). First dorsal interosseous (1DI), abductor digiti minimi (AbDM), flexor digitorum superficialis (FDS) and extensor digitorum communis (EDC) muscles were recorded using adhesive surface electrodes.

Cortical slow wave and single unit recordings, together with EMG data, were obtained from two monkeys (29 and 30), and quantitative analysis was carried out on data recorded from one of these monkeys (29). In this monkey, two glass-insulated platinum–iridium microelectrodes (impedance 500 kΩ to 1 MΩ at 1 kHz) were then inserted into the motor cortex using hydraulic microdrives, which allowed independent positioning of each electrode. The horizontal interelectrode distance was held constant at 1·5 mm. The electrodes were lowered until trains of intracortical microstimuli (ICMS, 13 pulses, 0·2 ms pulse width, 300 Hz) elicited EMG responses or overt movements of the hand or digits with a threshold less than 20 μA. The electrodes were then moved to search for pyramidal tract neurones, identified antidromically from the pyramidal electrodes using conventional criteria (Lemon *et al.* 1986).

Each electrode was connected to the inverting input of a head stage preamplifier (Neurolog NL100AK). The output from these was amplified (gain, 5 or 10K), and then filtered (Neurolog NL125). Filters were set to a bandpass of 10–120 Hz for the slow wave portion and 300 Hz to 10 kHz for spikes. The slow wave data were amplified by further DC amplifiers in some sessions. Spikes were recorded on a Racal Store 14 tape-recorder using direct record modules (300 Hz to 10 kHz); the slow waves were recorded using FM modules (DC to 600 Hz).

Off-line, cell spikes were discriminated into TTL pulses using a double amplitude–time window discriminator. Spike occurrence times were digitized by a PC-compatible computer fitted with 1401 Laboratory Interface (CED Ltd, Cambridge, UK), together with rectified EMG (sampled at 5 kHz) and the slow wave signals (sampled at 250 Hz).

Data were recorded from a total of ten penetrations in the two hemispheres of monkey 29. In monkey 30, slow wave recordings were made simultaneously from up to four sites separated by 300–1300 μm, using a 16-channel 'Eckhorn' drive (Thomas Recording Ltd, Marburg, Germany). Data from eleven penetrations were analysed. In the remaining four monkeys (which were used primarily for quite separate studies) only EMG data were available for analysis.

Following the end of the experimental period, the monkey was killed by an overdose (50 mg kg^{-1} I.V.) of pentobarbitone (Sagatal; Rhone Merieux, Harlow, UK) and perfused through the heart. The brain and spinal cord were removed for histological analysis.

Analysis

Local field potential spectral analysis. Analysis in the frequency domain, whilst mathematically equivalent to that in the time domain, serves to emphasize different features of the data, and is more appropriate when dealing with oscillatory data (Rosenberg, Amjad, Breeze, Brillinger & Halliday, 1989). Accordingly, the interactions between the slow wave recordings at different sites, and between slow wave and EMG, were assessed using spectral analysis. Two separate analyses were carried out. The first used all data recorded during an experiment, including all phases of task performance and periods in between successful trial performance. The objective was to characterize the frequency of oscillations. The second used sections of data selected according to the phase of task performance; this aided investigation of any task-related modulation of oscillatory activity.

The first analysis was performed as follows. For a single analog data channel, the power spectrum was calculated using a Fast Fourier Transform (FFT) algorithm (Press, Flannery, Teukolsky & Vetterling, 1989) with a 256 point window. In the case of the slow wave potentials, all FFT calculations were performed on the raw time series, sampled at 250 Hz. For the rectified EMG, which had been sampled at 5 kHz, the signal was smoothed by averaging successive sets of twenty points, producing a series also effectively

sampled at 250 Hz. Under these conditions, the maximum discernable frequency is 125 Hz (Nyquist Theorem; Press *et al.* 1989).

In order to measure the extent to which signals were correlated in the frequency domain, coherence was calculated (Farmer, Bremner, Halliday, Rosenberg & Stephens, 1993). This is a measure of the proportion of the signal within a particular frequency band which has a constant phase relationship between the two sources, and is bounded between 0 and 1. It was calculated as follows. If the FFT derived from signal i ($i = 1,2$) over the lth 256 point section ($l = 1...L$) is $F_{i,l}(f)$, then the cross-spectrum is:

$$X_{12}(f) = \frac{1}{L}\sum_{l=1}^{L} F_{1,l}(f)F_{2,l}^*(f), \tag{1}$$

where * denotes complex conjugate; both F and X are, in general, complex numbers. The autospectrum of one of the signals is given by an analogous expression:

$$A_i(f) = \frac{1}{L}\sum_{l=1}^{L} F_{i,l}(f)F_{i,l}^*(f). \tag{2}$$

The power spectrum is simply $|A_i(f)|^2$, and the coherence is given by:

$$C_{12}(f) = \frac{|X_{12}(f)|^2}{A_1(f)A_2(f)}. \tag{3}$$

Before calculating C_{12}, the cross-spectrum X_{12} and autospectra A_i were smoothed using a Hanning window in which each point was replaced with the weighted sum of its value and that of the two surrounding points, with weights 0·25, 0·5 and 0·25 (Farmer *et al.* 1993).

Significance of the coherence measures was estimated using the test provided by Rosenberg *et al.* (1989). On the null hypothesis that the two signals were independent, coherence above Z was considered significant at $P < \alpha$, where

$$Z = 1 - \alpha^{1/(L-1)} \tag{4}$$

and L is the number of disjoint sections used in the estimation of the auto- and cross-spectra in eqns (1) and (2).

In order to investigate how the coherence and power spectra varied during performance of the precision grip task, sections of data 2·048 s before and 1·024 s after the 'End hold' marker (see above) were used. These 768 sample series were split into twelve sections of sixty-four points each. The coherence and power were then calculated separately using the first section from all available trials, the second and so on, with an FFT length of sixty-four points. This allowed investigation of task-related changes in spectral measurements with a frequency resolution of 3·9 Hz and time resolution of 0·256 s. Measures were plotted as two-dimensional colour maps to aid visualization.

In addition to spectral analysis, time-domain analysis over all data recorded in a session was applied to those combinations of cortical potentials and EMGs which showed coherence peaks at around 20 Hz. This involved calculating the cross-correlation function $r(\tau)$:

$$r(\tau) = \frac{\dfrac{1}{t_{\max}}\sum_{t=0}^{t_{\max}} f_1(t)f_2(t - \tau) - \bar{f}_1\bar{f}_2}{\sigma_1\sigma_2}, \tag{5}$$

where f_1 and f_2 are the two signals to be analysed, $\bar{f}_1$ and $\bar{f}_2$ are their means and σ_1 and σ_2 are their standard deviations. So defined, r is bounded between -1 and 1. The time of the first peak of this function after time zero (with positive τ indicating EMG

lagging the cortical signal) was measured to estimate the time delays between the coherent portion of the two signals.

Spike-triggered averages of local field potentials. Local field potentials recorded as described above are effectively recordings of the mean postsynaptic potentials of cells in the vicinity of the electrode tip (Lemon, 1984). Spike-triggered averaging of these field recordings is expected to be a powerful means of revealing synchronous activity between the trigger cell and the neurones making synapses at the slow wave recording site (Murthy & Fetz, 1997b). Such averages in the present study frequently showed oscillations, in agreement with observations of Engel, Konig, Gray & Singer (1990) in visual cortex, where averages were compiled with multiunit activity as the trigger. A quantitative method was used, similar to the technique proposed by Engel *et al.* (1990).

Averages were compiled for a period 200 ms before and after the triggering spike. The standard error time course was also computed from the standard deviation time course, divided by the square root of the number of triggers. A Gabor function (Gabor, 1946) was fitted to the average using the Levenberg–Marquardt non-linear least-squares algorithm (Press *et al.* 1989); the algorithm took account of the standard error of each point. The function $G(t)$ had the form:

$$G(t) = k + B\exp[(t - t_0)^2/2\tau^2]\cos(2\pi(t - t_0)/T), \tag{6}$$

where B, k, T, τ and t_0 are parameters. Any fitting algorithm can suffer from the problem of local minima, which prevent it from reaching the true global minimum. In order to overcome this, the fitting was carried out in an interactive manner. The program implementing the Levenberg–Marquardt algorithm first carried out an initial fit, which was displayed along with the raw data. The parameters were adjusted manually, and a fit starting from these values was then calculated. This proceeded until the smallest value of the mean square error between data and fitted function was found; these final parameters were used in subsequent analysis.

The Levenberg–Marquardt algorithm calculates the covariance matrix C_{ij} for the fitted parameters. This was used to calculate the standard error $\sigma_G(t)$ in the value of the fitted Gabor function $G(t)$ as:

$$\sigma_G(t) = \sum_i \left(\sum_j \frac{\partial G}{\partial p_i} C_{ij} \frac{\partial G}{\partial p_j} \right), \tag{7}$$

where the five parameters of the Gabor function in eqn (6) have been rewritten as p_i ($i = 1...5$) for simplicity of notation. The nth peak of the Gabor function was considered significant if:

$$G(nT + t_0) - k > 2\sigma_G(nT + t_0). \tag{8}$$

This provided an objective means of assessing whether the average showed significant oscillations (i.e. whether eqn (8) held for $n = 1$, the first peak), and of how many cycles of the oscillation were present (the largest n for which eqn (8) was true).

The technique originally proposed by Engel *et al.* (1990) relies on the use of the fitted parameters alone; it has been criticized, since it is susceptible to false positives caused by the Gabor function providing a poor fit to the average (Young, Tanaka & Yamane, 1992). The present method overcomes this limitation, since use of the standard deviation of the fitted Gabor function naturally takes into account the goodness of fit. Thus, even fitted Gabor functions with large amplitude (high B) will fail to satisfy eqn (8) if the standard deviation is large, as it will be in the case of a poor fit. In each average analysed here, the results of the quantitative analysis were the same or more conservative than a subjective judgement of the number of peaks present.

RESULTS

## Synchronous oscillatory activity in slow wave recordings

Examination of the slow wave recordings often revealed bursts of oscillatory activity. Data from double-electrode recordings in monkey 29 which illustrated this are shown in Fig. 1. In this section of data, two bursts of oscillatory activity can be seen, occurring simultaneously on each electrode.

The oscillatory activity was quantified using spectral analysis techniques as described above. Figure 2 shows the results of such an analysis on the experimental session from which the data of Fig. 1 were taken. Figure 2A illustrates the power spectrum of the voltage in the two recordings. There are several peaks in these spectra. Two sharp peaks are evident at 50 and 100 Hz. These peaks are artefactual, and caused by contamination of the recordings by mains noise; such contamination is very difficult to avoid when the frequency range of interest is close to 50 Hz. A peak is also present at 4 Hz; however, this frequency was below the filter high-pass frequency, making interpretation unreliable. Finally, there is a broader, physiological peak at 21 Hz, which is present in the slow wave recordings from both sites.

Figure 2B plots the coherence between the slow waves recorded on the two electrodes. The 5% significance level for the coherence calculation in this case is 0·00139; all points plotted in Fig. 2B exceed this. This probably represents common signals recorded by the two electrodes from distant generators, as they were only separated by 1·5 mm. However, three clear peaks can be seen in the coherence. Two are, unsurprisingly, at 50 and 100 Hz – the source of most power at these frequencies is mains noise, which is common to both channels. However, there is also a much broader peak at 21 Hz. This represents oscillatory activity in both recordings with a constant phase relationship between the two.

Similar results were seen in all ten double-electrode penetrations available for analysis in monkey 29. Measurements from the nine penetrations where the peak was clear showed a mean frequency of 23·4 Hz (range, 21·0–27·8 Hz, measured from the middle of the frequency bin with largest coherence), with a mean peak coherence of 0·46 (range, 0·26–0·82). Slow wave recordings were made in both hemispheres of monkey 29, with data collected from the right hemisphere about 3 months after that on the left, after the animal had been retrained to perform the precision grip with the left hand. Examination of the data separately for each hemisphere indicated that the frequency at which the maximum coherence occurred between EMG and slow waves was slightly higher for right hemisphere recordings than for left (29·7 Hz compared with 22·1 Hz). This difference was significant ($P < 0·001$, Student's t test). In monkey 30, in which recordings were made only from the left hemisphere, the mean frequency of the oscillations, measured over the 9/15 pairs of recordings where a peak was visible, was 22·8 Hz.
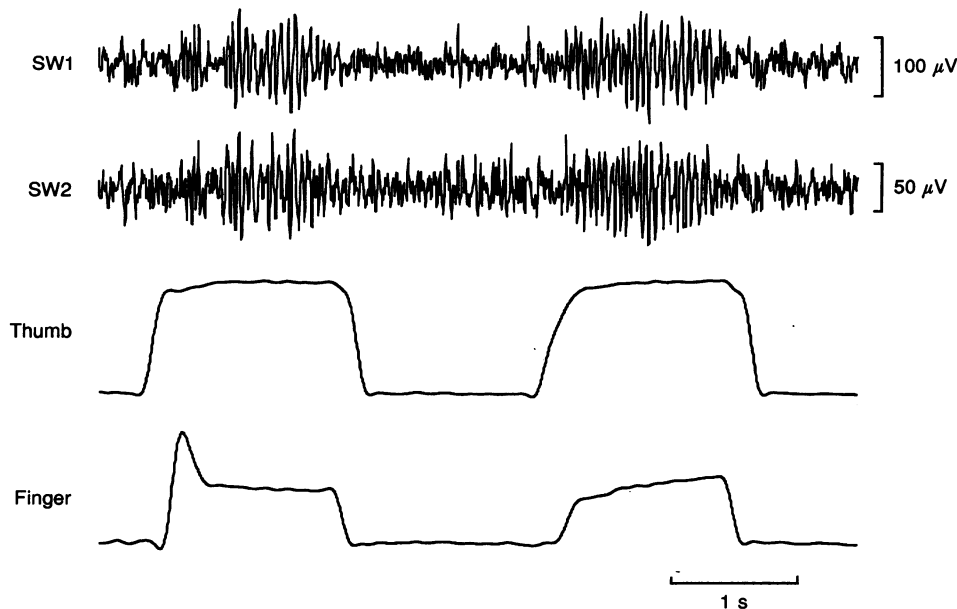
Figure 1. Synchronous slow wave oscillations during precision grip task

Example of a section of recording showing slow waves from two cortical sites (SW1 and SW2), together with the position of finger and thumb levers. Oscillations appear during the hold period of the task, which appear synchronous between the two sites. Data in this and subsequent figures are from monkey 29, unless otherwise specified.

Task-related modulation of cortical oscillations

Figure 1 suggests that the oscillations in slow wave activity occur at a well-defined part of the precision grip task, namely the hold period after the monkey has correctly positioned the levers and is waiting for a reward. This was investigated quantitatively by calculating the power spectra and coherence of the slow wave recordings as they varied relative to the task 'End hold' marker. Figure 3 shows an example of this calculation for the same experimental session as illustrated in Figs 1 and 2. Figure 3A and B plots the power in a particular frequency range *versus* time relative to 'End hold'. The frequency is given on the vertical axis, and peri-task time on the horizontal axis. Averages of the finger and thumb lever position traces are presented in Fig. 3D and E, respectively, for reference. All plots in Fig. 3 have the same horizontal scale, stretching from 2 s before to 1 s after 'End hold'.

Panels A and B in Fig. 3 show an increase in power around 20 Hz in the three bins (*ca* 0·75 s) prior to 'End hold', confirming the impression given by Fig. 1. Figure 3C plots the coherence between the two recordings. There is a similar peak in coherence at 20 Hz at the end of the hold period. The peaks in power and coherence at 50 and 100 Hz are less noticeable in Fig. 3 than in Fig. 2. This is because the 20 Hz peaks are much larger when only hold period data are analysed than when all available data are used. These larger

20 Hz peaks therefore overshadow the 50 and 100 Hz peaks on the colour scales used in Fig. 3.

In monkey 29, a similar task dependence of the cortical oscillations and their coherence was seen in eight of the other nine pairs of recordings available for analysis. Between 102 and 323 trials were available for analysis in these recordings. These results were confirmed in simultaneous cortical recordings from two primary motor cortex (M1) sites in a second animal (monkey 30). Cortical slow waves in the 20–30 Hz band were again maximal during the hold phase of the task; an example is shown in Fig. 7A.

Coherence between cortical slow wave and EMG activity

If the oscillatory activity recorded at the motor cortex affected cortical output neurones, oscillations in the amount of corticospinal tract activity would occur. This could cause oscillatory bursting of motoneurone firing, potentially detectable in the gross EMG (Murthy & Fetz, 1997a). Figure 4 presents a small section of recording where such bursting of the EMG could clearly be seen in the raw data. Figure 4A and B gives the slow wave recording from the two cortical sites; Fig. 4C presents the rectified, unsmoothed EMG from the AdP muscle. There are synchronous bursts of EMG which coincide with the negative phases of the slow wave oscillations.

Figure 2. Power spectra and coherence of two simultaneously recorded cortical slow waves

A, example of the power spectra of two simultaneously recorded cortical slow waves, shown overlaid in continuous and dotted lines. Peaks at 50 and 100 Hz are artefactual due to contamination by mains noise. Note the logarithmic scale. The bar indicates the region where the amplifiers had a flat frequency response. B, coherence between the two signals whose power is plotted in A. Artefactual peaks at 50 and 100 Hz are again present, but a physiological peak can be seen around 20 Hz. All values are above the theoretical 5 % significance limit, suggesting electrical cross-talk is present (see text). All available data from recordings at these sites were used in these calculations.
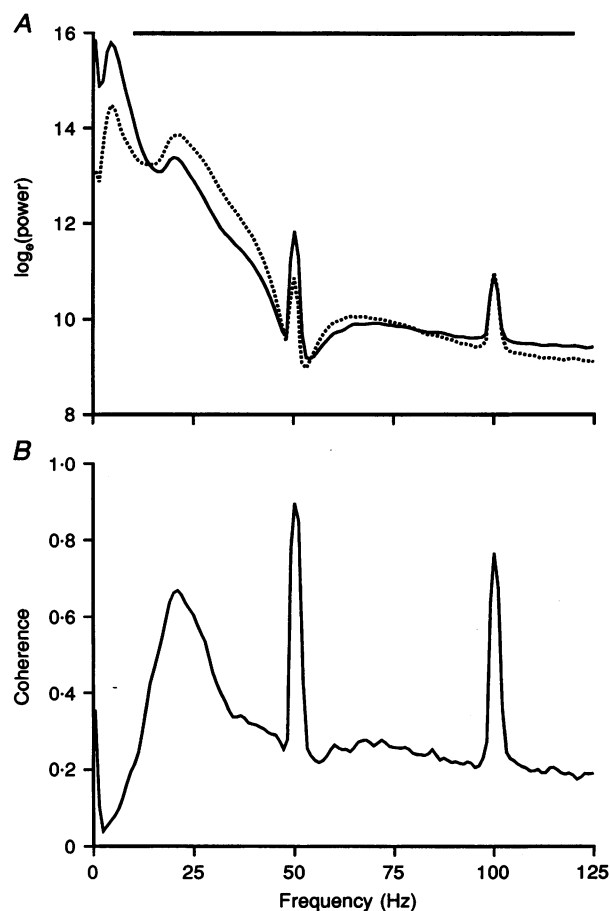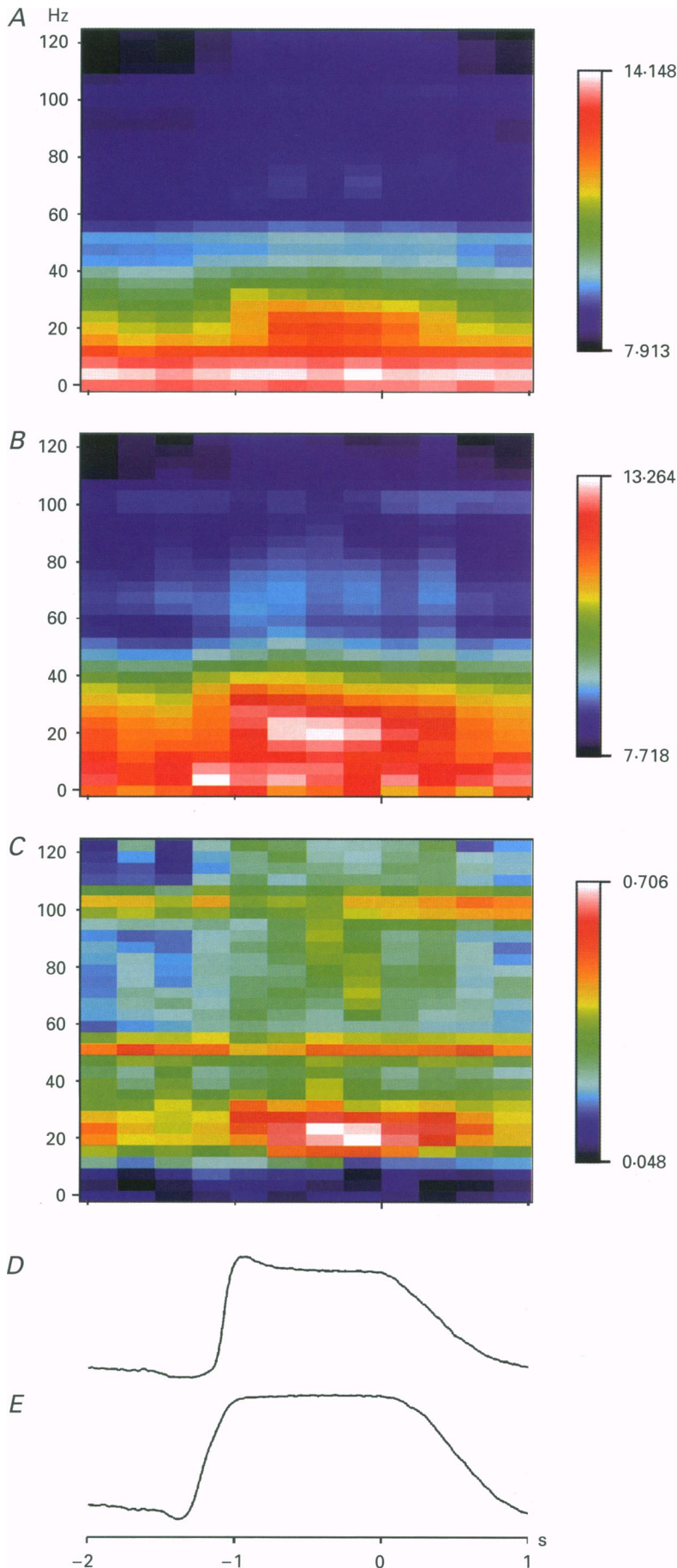
Figure 3. Example of variation in spectral measures with task performance

A and *B*, the logarithm to base e of the power in each slow wave signal (scale bars to the right of each figure). The vertical axis plots frequency and the horizontal axis plots time during task performance, relative to the 'End hold' task marker. Peaks at around 20 Hz can be seen in the hold period (−1 to 0 s relative to 'End hold'). *C*, the coherence between the two signals, illustrated in a similar way. The coherence peaks during the hold period at around 20 Hz. *D* and *E*, averages of finger and thumb positions, respectively, compiled with respect to the 'End hold' marker and shown on the same horizontal scale as *A–C*. Same experimental session as shown in Fig. 2. Compiled from 274 trials of the behavioural task.

Figure 5 provides quantitative measurements of this phenomenon for two muscles recorded in the same experiment. Panels on the left (Fig. 5A–C) show data from 1DI and those on the right show data (Fig. 5D–F) from AdP muscles. Figure 5A and D plots the power spectra of the EMG from these two muscles. A 20 Hz peak can be seen for AdP. In contrast to the cortical recordings, there is no evident 50 Hz mains contamination. This is probably explained by the much lower impedance of the EMG electrodes (< 10 kΩ), compared with the cortical electrodes (500 kΩ to 1 MΩ), leading to relatively clean EMG recordings. The coherence with the cortical slow wave recordings is illustrated in Fig. 5B and E (slow wave from site 1) and Fig. 5C and F (site 2). A dotted horizontal line marks the 5% significance level in each case. The large separation of the cortical and EMG recording sites eliminates electrical cross-talk, so that most points fail to show significant coherence, in contrast to the plots of Fig. 2. However, there are significant peaks close to 20 Hz for each of the four combinations of EMG with slow wave recording.

Shown as insets in Fig. 5B, C, E and F are the cross-correlations between the slow wave signal and the EMG, whose coherence is illustrated in the main part of the figure. These all show damped oscillations, with a period consistent with the coherence calculations.

The presence of a common oscillatory drive to muscles from the motor cortex implies that there should be coherence at 20 Hz between EMG recordings from different muscles. This was found to be the case, as illustrated in Fig. 5G. The close proximity of 1DI and AdP means that electrical cross-talk becomes a contaminant again, so that all points in Fig. 5G lie above the theoretical 5% significance level. However, a 20 Hz peak can be seen above the presumed artefactual coherence.

Changes in the coherent oscillatory activity in the EMG with task performance could also be discerned, as illustrated for the same session in Fig. 6; the design of this figure is intended to mirror that of Fig. 5. Data from 1DI are presented on the left, AdP on the right. Figure 6A and E shows averages of smoothed rectified EMG activity relative to the 'End hold' marker. The time scale again runs from 2 s before to 1 s after this marker, and is constant for all plots in Fig. 6. Panels B and F show the power spectra of the EMG from these two muscles, using a similar display to that of Fig. 3. As well as a generalized increase in power coincident with the peaks in EMG activity in each muscle, there is an increase in power in the 20 Hz region during the hold period (-1 to 0 s relative to 'End hold').

Figure 6C, D, G and H shows the coherence of the two EMGs with the two cortical slow wave recordings. The colour scale used has been adjusted to threshold out all coherence values below the 5% significance level. The 20 Hz coherence peak during the hold phase is readily apparent.

Figure 6I presents the coherence between the rectified EMG of 1DI and AdP as a function of time during the task. The 20 Hz coherence during the hold period can also be seen here. Similar patterns of coherence and task dependence were found in EMG data recorded from four other animals, although the precise time and frequency of maximum coherence varied between animals. An example is shown in Fig. 7B; there is again increased coherence in the hold period of the task.
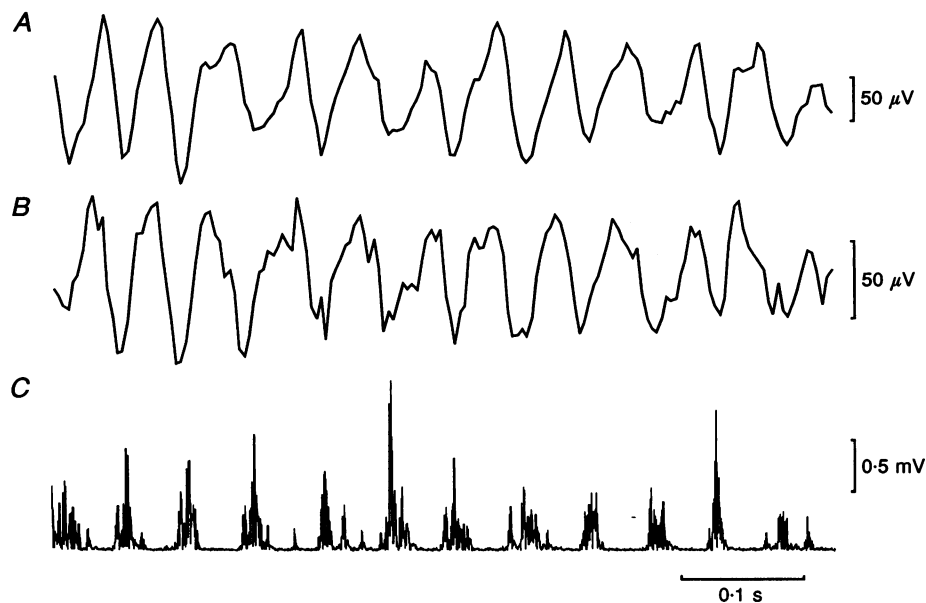
Figure 4. Slow wave recording from two cortical sites and EMG from AdP muscle

Section of raw recording showing two cortical slow waves simultaneously recorded (A and B), together with rectified EMG from the AdP muscle (C). Clear bursting behaviour is visible in the EMG, which appears in phase with the synchronous cortical oscillations.
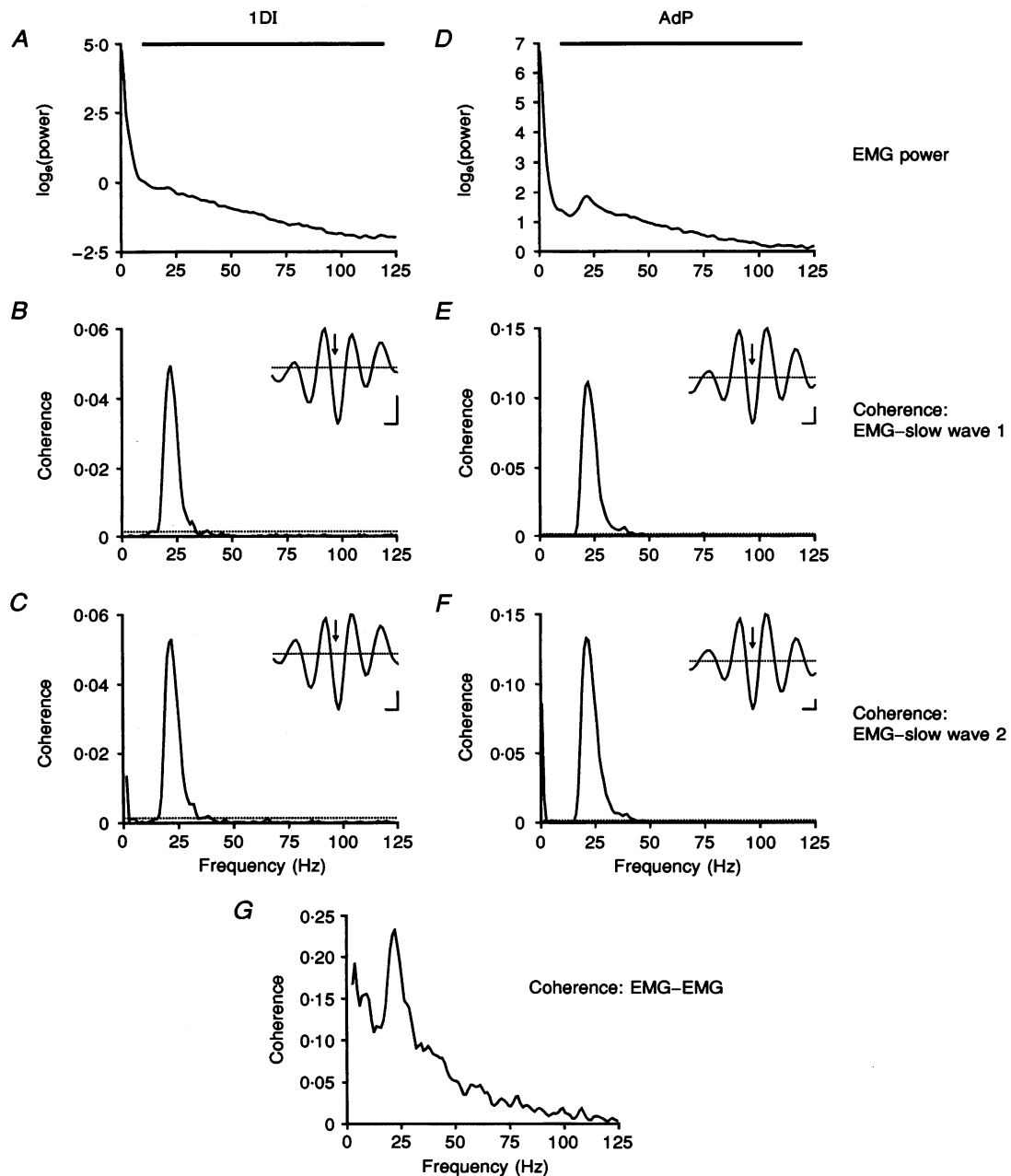
Figure 5. Spectral measures calculated from EMG recordings

A–C relate to the 1DI muscle, *D–F* to AdP. *A* and *D*, power spectra of the EMG. A peak at 20 Hz is visible in *D*. *B* and *E*, coherence with cortical slow wave recording from one site; *C* and *F*, coherence with cortical slow wave recording from the other site recorded during this session. Dotted lines mark the theoretical 5% significance level. Peaks at 20 Hz are present in all four recordings. Large values of coherence at 0 Hz (DC) have been excluded from these plots for clarity. The bar at the top of each column indicates the range where the amplifiers had a flat frequency response. Insets show cross-correlations calculated between the signals whose coherence is shown in the main part of the figure. Arrows show time of zero lag; dotted lines, the zero correlation level. Peaks to the right of the arrow indicate EMG lagging cortical recordings. Scale bars are 20 ms, $r = 0.01$. *G*, coherence between the 1DI and AdP EMG recordings. All points lie above the 5% significance limit (not shown); this is presumably due to electrical cross-talk between the two EMGs. A peak is visible, however, at 20 Hz. Same experimental session as Fig. 3. All available data from this recording session were used in this analysis.

In monkey 29, evidence for 20 Hz coherence between cortical slow waves and EMG was obtained in nine out of ten recording sessions. In twenty-nine combinations of slow wave and EMG activity, significant coherence could be seen both when the calculation included all data available (as in Fig. 5) and when the task relationship of the coherence was studied as in Fig. 6. Twenty-four instances were observed where significant coherence was only seen in one or the other of these calculations, of which sixteen showed a significant effect only in the task-dependent data. This is assumed to result from the different sensitivities of each method. Thus, including all the data may decrease the signal-to-noise ratio if long periods in which the monkey is not working are present, when presumably no oscillations occur.

In monkey 29 significant 20 Hz coherence was seen in 37/124 combinations of cortical slow wave recording and rectified EMG when all available data were used. The number of significant calculations for each muscle was: AbPB, 2/18; 1DI, 12/20; AdP, 13/18; AbDM, 4/20; EDC, 1/20; FDP, 1/10; FDS, 4/18. The extent of the peak was defined as the points where it crossed the 5% significance level; in the case where the significance level was crossed several times, the crossings either side of the coherence maximum were used. The mean onset frequency of the coherence peak, measured to the left of the frequency bin, was 20·9 Hz (range, 11·7–30·3 Hz), and the mean offset frequency, measured to the right of the frequency bin, was 32·7 Hz (range, 19·5–43·0 Hz). The mean peak frequency was 25·8 Hz (range, 18·1–34·7 Hz), with mean coherence at the peak of 0·025 (range, 0·00078–0·13).

Cross-correlation analysis on the thirty-seven combinations of slow wave and EMG recordings which showed 20 Hz coherence produced thirty-three cross-correlations in which a clear peak was visible at positive lags (EMG lagging slow waves). The mean lag of this peak was 20·8 ms (range, 4–46 ms). In monkey 30, coherence at 20–30 Hz was also seen between slow wave recordings and EMG, although this was rather less common and weaker than in monkey 29.

Timing of the coherence peak

The timing of the 20 Hz coherence peak relative to the task was determined from the forty-five pairs of EMGs with slow wave recording, where it was seen in the task-related plots. The onset occurred with a mean time of 0·72 s before 'End hold' (range, 0·26–1·0 s), the offset with a mean time of 0·065 s after 'End hold' (range, 0·51 s before to 0·77 s after). The timing of the peak could be determined in each case with an accuracy of only 0·26 s (the bin width in the task-related frequency plots). Examination of the timing of the coherence separately for each hemisphere showed a small but significant difference in the mean onset time (0·65 s for left hemisphere compared with 0·82 s for right, $P < 0.05$, Student's t test), but no significant difference in offset time.

Table 1. Relationship between slow wave–EMG coherence and ICMS responses

	ICMS response	No ICMS response	Total
Coherence	24 (17·1)	29 (35·9)	53
No coherence	16 (22·9)	55 (48·1)	71
Total	40	84	124

Contingency table illustrating the relationship between responses in a muscle to stimulation of a cortical site and the presence of significant 20 Hz coherence between the cortical recording and the muscle EMG. Values in parentheses give the expected occurrences on the null hypothesis of no interaction between the presence of ICMS and coherence. A χ^2 test shows significant deviation from this null hypothesis ($P < 0.01$).

Coherence at low threshold intracortical microstimuli (ICMS) sites

If the cortico-motoneuronal (CM) system mediates the coherence between oscillations in cortical slow wave and EMG, a correlation might be expected between the presence of such coherence and evidence that neurones at the recording site project to the motoneurone pool of that muscle. This was tested in monkey 29 as follows. A slow wave recording and EMG were classed as showing 20–30 Hz coherence if they showed it either in overall coherence plots or in those compiled relative to the 'End hold' marker. Neurones at the site were assumed to make functional connections with motoneurones supplying the muscle if responses in that EMG to trains of ICMS had been seen with threshold less than 20 μA during the initial electrode placement (see Lemon *et al.* 1986). Such a classification produced the contingency table shown in Table 1.

A χ^2 test on the data of Table 1 rejected the null hypothesis of no interaction between the two categories at the 1% level. Sites capable of facilitating a muscle when stimulated therefore have a tendency also to show coherence with the EMG of that muscle, although this relationship does not hold invariably.

Spike-triggered averages (STAs) of slow wave recordings

In monkey 29, a total of eighteen pyramidal tract neurones (PTNs) were recorded simultaneously with cortical slow waves, yielding seventeen STAs of the slow wave recorded at the same site and seventeen STAs of the slow wave at the distant site. Figures 8 and 9 illustrate the finding for two cells.

Figure 8*A* and *B* illustrates the identification of the two PTNs, which were simultaneously recorded on the same electrode and separated on the basis of differences in the size and shape of their action potentials (Fig. 8*A*). Figure 8*C*
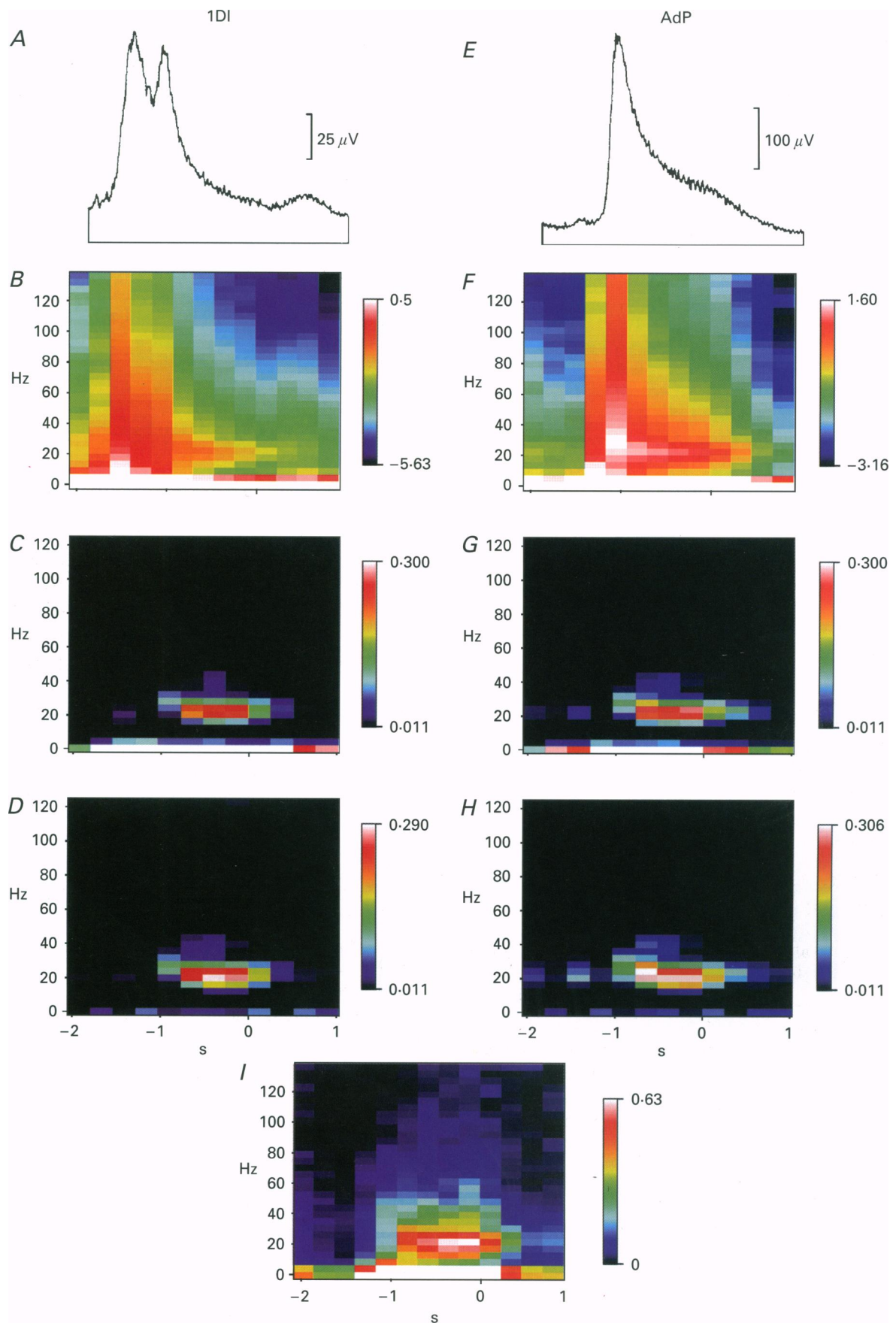
Figure 6. For legend see facing page.

shows the autocorrelograms of the two cells. No periodic features are visible in either of these. As shown in Fig. 8D, the firing rate of the two cells modulated differently during task performance.

Figure 9A illustrates the STAs of the cortical slow wave recorded from the same site as the cell spikes; Fig. 9B shows the STAs of the slow wave recorded from the distant site. In each case, there are oscillations in the averages, indicating that the neurone spike train was partially phase locked to the slow wave oscillations. The dotted lines superimposed on the STAs give the fitted Gabor functions, as described in Methods. These are a relatively good fit to the central portions of the average; the fit becomes less good at the edges. In part this is due to the asymmetric nature of the oscillations. In Fig. 9B, oscillations are stronger to the left of the spike (marked by the dashed line) than to the right. This is probably a result of the non-stationarity of both spike and slow wave data, which vary in a task-dependent fashion.

Since the PTNs illustrated in Figs 8 and 9 are partially phase locked to the slow wave oscillations, and the cortical oscillations show significant coherence with certain EMGs (Figs 5 and 6), it might be expected that STAs of these EMGs would show oscillations. Figure 9C and D shows that this was indeed the case for the 1DI and AdP muscle, for both neurones illustrated. All spikes recorded from these cells were used in the compilation of these averages; the size of the largest peak was 10·5–14·7% of the background level in these averages. Oscillatory STAs were not always seen, presumably because of their small size, representing the convolution of a partial phase locking of the cell to the cortical oscillations, and a weak coherence between cortical oscillations and EMG. Such small oscillatory peaks can easily disappear into the noise of the STA, particularly since in averages of rectified EMG small signals tend to be underestimated (Baker & Lemon, 1995).

As noted above, the two neurones shown in Figs 8 and 9 showed little evidence of periodic firing in their autocorrelograms. A similar lack of sub-peaks in the autocorrelogram was also seen when the autocorrelograms were compiled from spikes selected from only the hold period of the task. This was not true for all PTNs investigated, many of which had at least one secondary peak in the autocorrelogram. However, the two cells illustrated here show that this is not a necessary condition for a cell to be

phase locked, on average, with the local field potential oscillations.

Eleven of the seventeen STAs of slow waves recorded from the same electrode as the triggering spike, and eleven of the seventeen STAs of distant slow waves, showed significant oscillatory activity defined relative to the fitted Gabor function. Out of the eighteen PTNs analysed, fifteen showed oscillations in at least one slow wave STA. The mean number of significant peaks either side of the origin in the twenty-two averages showing oscillations was 1·8 (range, 1–4). This is likely to be an underestimate, however, due to the asymmetric nature of the oscillations, which often resulted in the fitted Gabor function having fewer peaks than were apparent in the raw average. The period of the oscillations had a mean of 45·8 ms (range, 28·0–56·4 ms), corresponding to a frequency of 21·8 Hz. This is within the frequency range of the coherence peaks described above.

DISCUSSION

The present data confirm the presence of slow wave oscillations in primary motor cortex of the monkey and the coherence of signals recorded at remote sites in the 20–30 Hz bandwidth. We demonstrate two additional important features: first we have shown, by spike-triggered averaging, that pyramidal tract neurones contribute to the oscillations. Secondly, that the coherent oscillations in the 20–30 Hz region between cortical slow wave activity and EMG in contralateral hand muscles undergo very marked modulation during the different phases of the precision grip task.

Nature of the oscillations and coherence

The cortical oscillations that we have recorded have a similar bandwidth to those reported previously (Murthy & Fetz, 1992, 1997a; Sanes & Donoghue, 1993). The striking coherence at 20 Hz between the oscillations recorded simultaneously at different sites within M1 seems unlikely to have resulted from the activity of an oscillating generator distant from the electrodes at these sites. Clearly the electrodes, separated by only 1·5 mm, did record common signals, as shown by the significant coherence at all frequencies (see Fig. 2B). However, the coherence plots showed peaks around 20 Hz, which rose above the coherence at both lower and higher frequencies. A monotonic relationship of coherence with frequency would be expected if it

Figure 6. Changes in spectral measures derived from EMG with task performance

A–D relate to recordings from 1DI, *E–H* from AdP. *A* and *E*, averages of smoothed, rectified EMG compiled with the 'End hold' task marker as trigger (time 0). *B* and *F*, change in power of EMG with task performance. Peaks at 20 Hz during the hold period can be seen. *C* and *G*, coherence of EMG with slow wave recorded at one site, and *D* and *H* at the other site, as a function of task performance. Clear task dependence of the 20 Hz coherence is seen and primarily occurs during the hold period. Colour scales have been adjusted to threshold out all non-significant values of coherence. *I*, modulation of coherence between 1DI and AdP EMG with task performance. The 20 Hz peak can be seen during the hold period even when calculated between the two EMGs. All measurements were compiled from 274 trials of the behavioural task. The time scale is the same for all panels, running from 2 s before to 1 s after the 'End hold' marker.
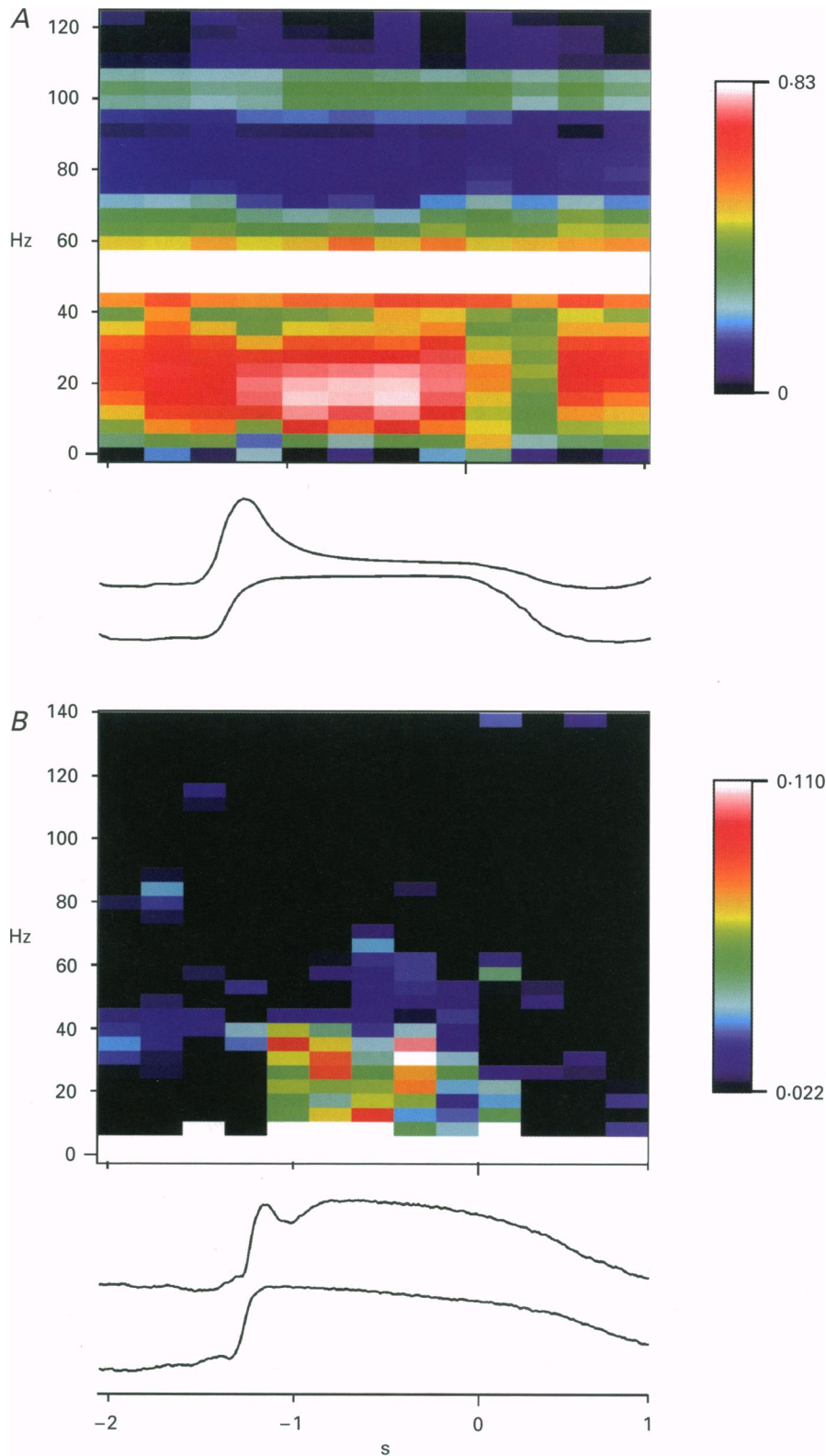
Figure 7. Examples of task-dependent coherence peaks recorded in two different monkeys performing the precision grip task

Display conventions as in Fig. 6*I*. *A*, coherence between two cortical slow wave recordings, separated by 600 μm (monkey 30). *B*, coherence between muscles AdP and AbDM (monkey 29). Averages of lever position compiled relative to the 'End hold' marker are shown beneath each plot (finger above thumb). The precise timing and frequency band of the coherence varies between animals, presumably as a result of different motor strategies for performing the task; however, there is broad similarity in the general finding. $n = 131$ trials in *A*; $n = 133$ trials in *B*.

were due solely to spread of potentials. Steriade, Amzica & Contreras (1996) estimated the spread of cortical potentials by showing that slow wave oscillations recorded in the grey matter were strongly attenuated when the electrode moved into the white matter, a distance of 1·6 mm. Murthy & Fetz (1997*a*) have demonstrated phase reversal of oscillatory local field potentials within the cortical grey matter, suggesting an intracortical origin. Secondly, coherence in the 20 Hz region was unambiguously seen between cortical recordings and EMG, such that it rose above the theoretical significance level only in this frequency band. Pairs of cortical sites both showed this coherence with the same EMG (see Fig. 5). Finally, the cortical coherence peaks modulated in a task-dependent manner, which would not be the case with a purely electrical phenomenon.

Most of the evidence for coherence at 20–30 Hz between cortical oscillations and EMG activity was obtained from one monkey, in which oscillatory activity was particularly

marked. However the same general results were confirmed in recordings from other animals, although the strength of coherence varied from one to another. This may represent a genuine difference between individuals in the extent to which oscillatory activity is generated by the motor cortex; it could also reflect the particular pattern of muscle activity adopted by each monkey in order to perform the task. Coherence can only be seen in muscles which show activity coincident with the presence of cortical oscillations, i.e. in the hold period.

The presence of coherence provides evidence of synchrony between remote cortical sites. It is in marked contrast to the failure of several authors to show significant cross-correlation peaks between single unit spikes recorded at such large inter-electrode spacings within motor cortex (Kwan, Murphy & Wong, 1987; Smith, 1989; Baker, Olivier & Lemon, 1994). The higher sensitivity of the slow wave coherence compared with single unit cross-correlation probably results from two
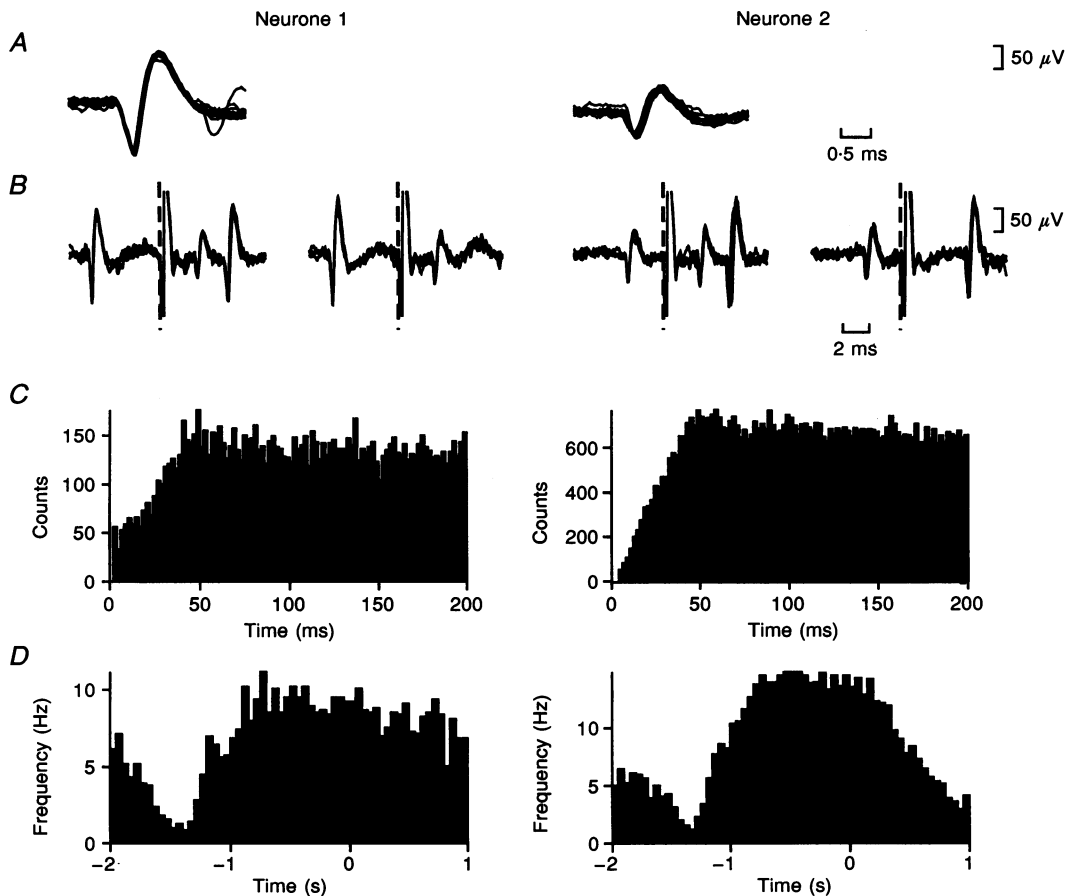

Figure 8. Example of spike data from two cells recorded simultaneously by the same electrode

A, overlaid spike waveforms showing the difference in amplitude which allowed reliable discrimination. *B*, collision test. Each sweep shows the cortical spike recording following stimulation through the chronically implanted pyramidal electrodes (dashed line). The stimulus was triggered at a delay after a spike occurred. In the left-hand panels, this delay was just before the critical delay, and an antidromic response can be seen. In the right-hand panels, the delay was 0·1 ms shorter, and the antidromic spike has been collided. *C*, autocorrelograms of neurone spikes. No periodicity is evident. *D*, firing modulation of the neurones with task performance. Response histograms are aligned to the 'End hold' task marker (time 0 s). *n* = 274 trials of the task.

factors. Firstly, the slow wave is most directly related to synaptic potentials, not cell firing. It therefore will detect effects even when they are subthreshold. Secondly, the slow wave is the average of the synaptic input to a large number of cells close to the recording electrode, such that the signal-to-noise ratio is improved by spatial averaging as well. Thus, coherence between the slow wave recordings is a highly sensitive measure of synchrony between two sites. However,
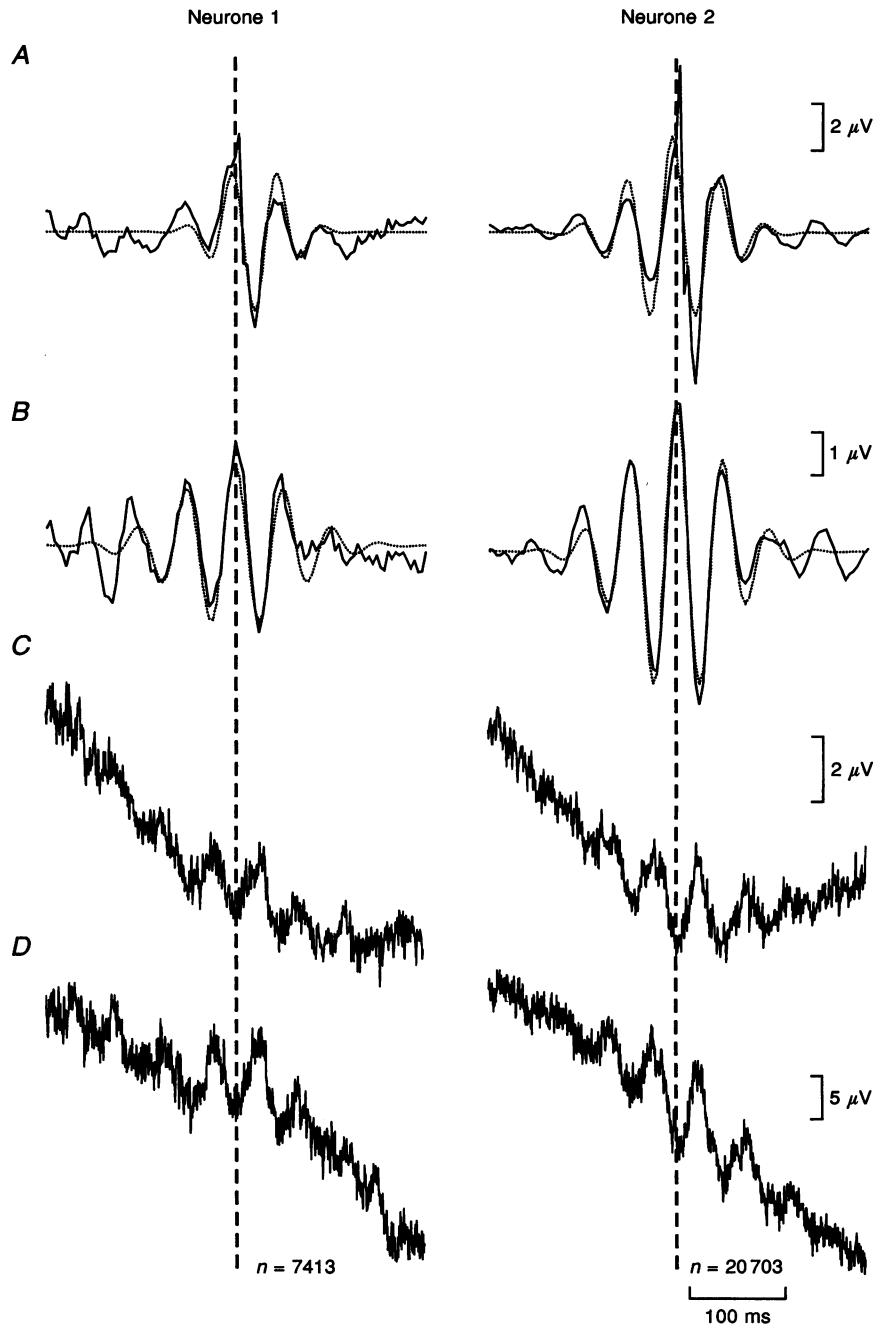
Figure 9. Spike-triggered averages of the cortical slow waves and EMGs

STAs of the slow wave signal extracted from the electrode used to record the spikes (A) and from the electrode 1·5 mm from this site (B). The same neurones as in Fig. 8. The STA is shown by a continuous line; the dotted line marks the best-fit Gabor function used to test significance of oscillatory peaks. In A, an artefact is present at the time of the triggering spike, due to low frequency components of the action potential appearing in the slow wave recording. C and D, spike-triggered averages of rectified EMG from 1DI and AdP muscles, respectively. Oscillations can be seen superimposed on slow changes in mean EMG level caused by non-stationarity of spike and EMG data. Dashed lines mark spike times. n gives the number of spikes used to compile the average. All available spikes were used in the compilation of these averages.

it cannot measure the size of the synchronous input to the two sites as a proportion of the total input, as is possible with single unit cross-correlograms. The slow wave potential is averaged over all cells at the site, and so necessarily represents only the synchronous synaptic input.

It is important to distinguish between the finding of coherence between distant cortical sites and the presence of oscillations. Power in the 20–30 Hz region must be present in order to measure coherence within this bandwidth. However, this does not indicate that the connections mediating coherence are only functionally important when oscillations appear. It is quite possible that the connections which serve to synchronize cell assemblies during oscillatory bursts could act in an asynchronous mode at other times. This would have no effect on slow wave coherence, but could be of great importance in patterning the discharge of individual neurones.

Coherent activity in the cortical output and its impact on target muscles

The presence of coherence between the cortical recordings and the EMG suggests that cortical output neurones receive the common input represented by the slow wave coherence. This is supported by the finding that spike-triggered averages of the slow wave compiled from the discharge of identified PTNs show clear oscillations (see Fig. 8). Thus, these oscillations could act as a component of the descending command to recruit motoneurones (Murthy & Fetz, 1997a). This command is mediated, in part, by changes in the firing rate of CM cells. However, the presence of synchronous oscillations in the CM outflow would act as a stronger input to recruit motoneurones than an asynchronous command having the same overall firing rate (Murthy & Fetz, 1994). The appearance of the 20–30 Hz oscillations in motor unit firing would be expected to have little consequence for motor performance, since they would be largely smoothed out by the twitch time of single motor units and the biomechanics of the limb. In this case, the oscillations might represent an efficient means of maintaining a tonic drive to motoneurones with as little CM activity as possible (see below). A characteristic feature of many identified CM neurones is their relatively slow firing rate during the hold period when compared with other phases of the task (Bennett & Lemon, 1996).

The presence of oscillations at 20–30 Hz could relate to an observation of Lemon & Mantel (1989). In that study, spike-triggered averaging of rectified EMG was performed using CM cell spikes which were selected according to the preceding and succeeding interspike interval. Unsurprisingly, short intervals gave a large postspike facilitation (PSF), probably due to summation and facilitation at the CM synapse (Porter, 1970). However, spikes with a preceding interval of 30–70 ms produced a larger PSF than those with an interval of around 20–30 ms. It could be that the longer intervals often represented spikes where the CM cell discharged in phase with cortical oscillatory activity. More synchronous

discharges from other CM cells would then be expected than when the cell fired at random, which could produce the increased PSF seen. It is interesting to note that the PSFs compiled with long preceding intervals were broader than those in STAs compiled with short interval spikes, in agreement with the suggestion that synchrony may be contributing more to these than to the short interval PSFs.

This report is the first to describe oscillatory STAs of rectified EMG activity triggered by PTNs. These features are obviously due to synchrony effects, and should not be confused with the postspike facilitations seen in such STAs and usually taken as evidence for CM connections (Fetz & Cheney, 1980; Lemon *et al.* 1986). The latter are much sharper, and have latencies consistent with conduction delays in the CM pathway (Porter & Lemon, 1993). STAs are usually shown on a faster time scale than those in Fig. 9*C* and *D*, so that oscillatory sub-peaks will not always be visible. However, the averages of Fig. 9*C* and *D* would still be classified as a synchrony PSF, due to their slow rise time, broad peak and early onset (Fetz & Cheney, 1980).

The finding of cortical and muscle coherent activity confirms that of Conway *et al.* (1995), who found coherence in the 14·5–28 Hz bandwidth between MEG recordings and hand muscle EMG in human subjects maintaining a steady contraction of the 1DI muscle. This coherence was present only between MEG recordings directly over the primary motor cortex, and with contralateral but not ipsilateral 1DI EMG.

Functional significance of the cortical oscillations

With a mean of 23·4 Hz, the oscillations reported here are similar to those at 25–35 Hz found by Murthy & Fetz (1992, 1997a,b) in monkey motor cortex, although there are differences in frequency and timing of coherence between animals (see Fig. 7), and even in the same animal between data recorded from left and right hemispheres. It is possible that the lower frequency of oscillations in the motor cortex, compared with the 40 Hz oscillations seen in the visual cortex (Engel *et al.* 1990; Eckhorn, 1994) reflects differences in their functional significance in motor *versus* visual cortical areas. It is indeed rather unlikely that oscillations subserve a single function within the cerebral cortex.

Our results show that coherent oscillations are particularly pronounced during the hold period of the precision grip task; Murthy & Fetz (1997a) also reported oscillations to be present during the hold period of a wrist extension–flexion task, although they were far less common during this highly overtrained task than when the monkey used a precision grip to retrieve small food rewards. Sanes & Donoghue (1993) reported oscillations to be most common while the monkey held the wrist or digits in a precued position, whilst awaiting the instruction to move to a new position; oscillations disappeared at the onset of movement. This may be comparable to our task, in that the monkey must maintain the hold period positions until a tone indicates completion of a successful trial and cues release of the levers.

The simplest explanation for the appearance of oscillatory bursts is that they represent an epiphenomenon. Murthy & Fetz (1997a) concluded that oscillations 'have no reliable relation to particular components of the movement and therefore seem unlikely to be involved directly in movement execution'. In our experience, the hardest part of training an animal is teaching it to squeeze the manipulandum levers gently into the target zone, rather than pressing them up against the end stops. Once this is learnt, sudden increases in the length of the hold period are well tolerated. This suggests that oscillations may occur when the motor cortex is 'resting' between the demanding tasks of positioning the digits within the target zone and removal of the hand at the end of the trial. If this is the case, oscillations could be considered as a stable dynamic state which can be held without excessive computational effort, and this might be advantageous for the maintenance of relatively stable motor states, such as a steady grip force to hold an object. Murthy & Fetz (1992) also noted the strong link between finger movements and oscillatory bursts (cf. Fig. 1). The presence of oscillations during precision grip but not during the wrist flexion–extension (Murthy & Fetz, 1992) may reflect the demands of the more demanding precision grip task and increased level of attention that is required (Murthy & Fetz, 1997a).

An alternative proposal, suggested by Engel, Konig, Kreiter, Schillen & Singer (1992), is that oscillatory activity could be used as a 'carrier wave' capable of transmitting information reliably via weak cortical connections. However, this proposal implies that neurones can only respond effectively to inputs at quantized time intervals every 50 ms or so, which would seem to prevent rapid processing of information. If this were true, it is also hard to understand why the oscillations occur during the hold period, when probably the most demanding parts of the task are just before and just after it.

The appearance of oscillations preferentially during the hold period of the task may relate to the results of our recent study using transcranial magnetic stimulation (TMS; Baker et al. 1995). Using the same precision grip task, it was reported that the descending corticospinal volley following TMS modulated during task performance and was largest during the hold phase. Previous studies on this task have shown that corticospinal cell firing rate is greatest in the pre-hold movement phase (Lemon et al. 1986; Bennett & Lemon, 1996). It is possible that the oscillations in the membrane potential of corticospinal cells interact with current induced by TMS to produce a mean increase in the size of the descending volley, compared with the situation when no oscillations are present. This would explain why the period of maximal corticospinal excitability does not coincide with the greatest corticospinal activity.

Wessberg & Vallbo (1995) have also recently provided evidence for a 'pulsatile motor command'. Their work concerns oscillations at 8–10 Hz, not the higher 20–30 Hz found here, and so may involve a different system. However, 8–10 Hz is the firing rate of motoneurones during weak

contractions (Milner-Brown, Stein & Yemm, 1973), and it is possible that in some circumstances motoneurone discharge could be phase locked by a higher frequency input from the cortex by, for example, responding every second or third cycle. In this way, cortical oscillations at 20–30 Hz could produce the type of pulsatile motor output seen by Wessberg & Vallbo (1995).

The frequency of oscillations reported here agrees well with estimates of the frequency of the 'temporal oscillator' proposed by Treisman, Faulkner, Naish & Brogan (1990) to underlie time perception, and by Treisman, Faulkner & Naish (1992) to play a role in the timing of motor outflow. These experiments studied the effect of giving auditory clicks at different frequencies on time estimation or movement times, and used a model of the expected interference between auditory input and the central oscillator to predict the oscillator frequency. The close agreement between the results of these psychological studies and the current data supports the idea that these oscillations are a pervasive feature of the nervous system.

In conclusion, the results reported here have shown the presence of oscillations which are synchronized across different sites in the motor cortex. These encompass the pyramidal tract neurones and even propagate to the EMG of some muscles active at the time of the cortical oscillatory bursts. Oscillations show a clear tendency to appear preferentially during the hold period of the precision grip task used here, but their function remains a matter of speculation.

BAKER, S. N. & LEMON, R. N. (1995). Non-linear summation of responses in averages of rectified EMG. Journal of Neuroscience Methods 59, 175–181.

BAKER, S. N., OLIVIER, E. & LEMON, R. N. (1994). Cross correlations between pairs of identified cells in monkey motor cortex: implications for the origin of post spike facilitation in rectified EMG of hand muscles. Society for Neuroscience Abstracts 20, 403.7.

BAKER, S. N., OLIVIER, E. & LEMON, R. N. (1995). Task-related variation in corticospinal output evoked by transcranial magnetic stimulation in the macaque monkey. Journal of Physiology 488, 795–801.

BAKER, S. N., OLIVIER, E. & LEMON, R. N. (1996). 20 Hz coherent oscillations in cortical and EMG recordings from a monkey performing a precision grip task. Journal of Physiology 494.P, 64–65P.

BENNETT, K. M. B. & LEMON, R. N. (1996). Corticomotoneuronal contribution to the fractionation of muscle activity during precision grip in the monkey. Journal of Neurophysiology 75, 1826–1842.

CONWAY, B. A., HALLIDAY, D. M., FARMER, S. F., SHAHANI, U., MAAS, P., WEIR, A. I. & ROSENBERG, J. R. (1995). Synchronization between motor cortex and spinal motoneuronal pool during the performance of a maintained motor task in man. Journal of Physiology 489, 917–924.

ECKHORN, R. (1994). Oscillatory and non-oscillatory synchronizations in the visual-cortex and their possible roles in associations of visual features. Progress in Brain Research 102, 405–426.

ENGEL, A. K., KONIG, P., GRAY, C. M. & SINGER, W. (1990). Stimulus-dependent neuronal oscillations in cat visual-cortex – intercolumnar interaction as determined by cross-correlation analysis. *European Journal of Neuroscience* **2**, 588–606.

ENGEL, A. K., KONIG, P., KREITER, A. K., SCHILLEN, T. B. & SINGER, W. (1992). Temporal coding in the visual cortex: new vistas on integration in the nervous system. *Trends in Neurosciences* **15**, 218–227.

FARMER, S. F., BREMNER, F. D., HALLIDAY, D. M., ROSENBERG, J. R. & STEPHENS, J. A. (1993). The frequency content of common synaptic inputs to motoneurones studied during voluntary isometric contraction in man. *Journal of Physiology* **470**, 127–155.

FETZ, E. E. & CHENEY, P. D. (1980). Postspike facilitation of forelimb muscle activity by primate corticomotoneuronal cells. *Journal of Neurophysiology* **44**, 751–772.

GABOR, D. (1946). Theory of communication. *Journal of the Institute of Electrical Engineers* **13**, 429–441.

KWAN, H. C., MURPHY, J. T. & WONG, Y. C. (1987). Interaction between neurons in precentral cortical zones controlling different joints. *Brain Research* **400**, 259–269.

LEMON, R. N. (1984). *Methods for Neuronal Recording in Conscious Animals. IBRO Handbook Series: Methods in Neurosciences.* Wiley, London.

LEMON, R. N. & MANTEL, G. W. H. (1989). The influence of changes in the discharge frequency of corticospinal neurones on hand muscles in the monkey. *Journal of Physiology* **413**, 351–378.

LEMON, R. N., MANTEL, G. W. H. & MUIR, R. B. (1986). Corticospinal facilitation of hand muscles during voluntary movement in the conscious monkey. *Journal of Physiology* **381**, 497–527.

MILNER-BROWN, H. S., STEIN, R. B. & YEMM, R. (1973). Changes in firing rate of human motor units during linearly changing voluntary contractions. *Journal of Physiology* **230**, 371–390.

MURTHY, V. N. & FETZ, E. E. (1992). Coherent 25- to 35-Hz oscillations in the sensorimotor cortex of awake behaving monkeys. *Proceedings of the National Academy of Sciences of the USA* **89**, 5670–5674.

MURTHY, V. N. & FETZ, E. E. (1994). Effects of input synchrony on the firing rate of a 3-conductance cortical neuron model. *Neural Computation* **6**, 1111–1126.

MURTHY, V. N. & FETZ, E. E. (1997*a*). Oscillatory activity in sensorimotor cortex of awake monkeys: synchronization of local field potentials and relation to behavior. *Journal of Neurophysiology* **76**, 3949–3967.

MURTHY, V. N. & FETZ, E. E. (1997*b*). Synchronization of neurons during local field potential oscillations in sensorimotor cortex of awake monkeys. *Journal of Neurophysiology* **76**, 3968–3982.

PORTER, R. (1970). Early facilitation at corticomotoneuronal synapses. *Journal of Physiology* **207**, 733–745.

PORTER, R. & LEMON, R. N. (1993). *Corticospinal Function and Voluntary Movement*, pp. 157–160. Oxford University Press, Oxford.

PRESS, W. H., FLANNERY, B. P., TEUKOLSKY, S. A. & VETTERLING, W. T. (1989). *Numerical Recipes: the Art of Scientific Computation.* Cambridge University Press, Cambridge.

ROSENBERG, J. R., AMJAD, A. M., BREEZE, P., BRILLINGER, D. R. & HALLIDAY, D. M. (1989). The Fourier approach to the identification of functional coupling between neuronal spike trains. *Progress in Biophysics and Molecular Biology* **53**, 1–31.

SANES, J. N. & DONOGHUE, J. P. (1993). Oscillations in local-field potentials of the primate motor cortex during voluntary movement. *Proceedings of the National Academy of Sciences of the USA* **90**, 4470–4474.

SINGER, W. & GRAY, C. M. (1995). Visual feature integration and the temporal correlation hypothesis. *Annual Review of Neuroscience* **18**, 555–586.

SMITH, W. S. (1989). Synaptic interactions between identified motor cortex neurons in the active primate. PhD Thesis, University of Washington.

STERIADE, M., AMZICA, F. & CONTRERAS, D. (1996). Synchronization of fast (30–40 Hz) spontaneous cortical rhythms during brain activation. *Journal of Neuroscience* **16**, 392–417.

TREISMAN, M., FAULKNER, A. & NAISH, P. L. N. (1992). On the relation between time perception and the timing of motor action: evidence for a temporal oscillator controlling the timing of movement. *Quarterly Journal of Experimental Psychology* **45A**, 235–263.

TREISMAN, M., FAULKNER, A., NAISH, P. L. N. & BROGAN, D. (1990). The internal clock: evidence for a temporal oscillator underlying time perception with some estimates of its characteristic frequency. *Perception* **19**, 705–743.

WESSBERG, J. & VALLBO, A. K. (1995). Coding of pulsatile motor output by human muscle afferents during slow finger movements. *Journal of Physiology* **485**, 271–282.

YOUNG, M. P., TANAKA, K. & YAMANE, S. (1992). On oscillating neuronal responses in the visual-cortex of the monkey. *Journal of Neurophysiology* **67**, 1464–1474.

Acknowledgements

Author's present address

E. Olivier: UCL 5449, Laboratory of Neurophysiology, University of Louvain, Avenue Hippocrate, 54, B-1200, Brussels, Belgium.

Author's email address

S. N. Baker: snb11@cam.ac.uk